Electronic Supplementary Material (ESI) for Journal of Materials Chemistry C.

SUPPORTING INFORMATION

Title: Colloidally stable, magnetoresponsive liquid crystals based on clay nanosheets

Author(s): Olena Khoruzhenko, Daniel R. Wagner, Sebastian Mangelsen,* Martin Dulle, Sabine Rosenfeldt, Volodymyr Dudko, Katharina Ottermann, Georg Papastavrou, Stephan Förster, Wolfgang Bensch* and Josef Breu *

SAXS data for double stacks

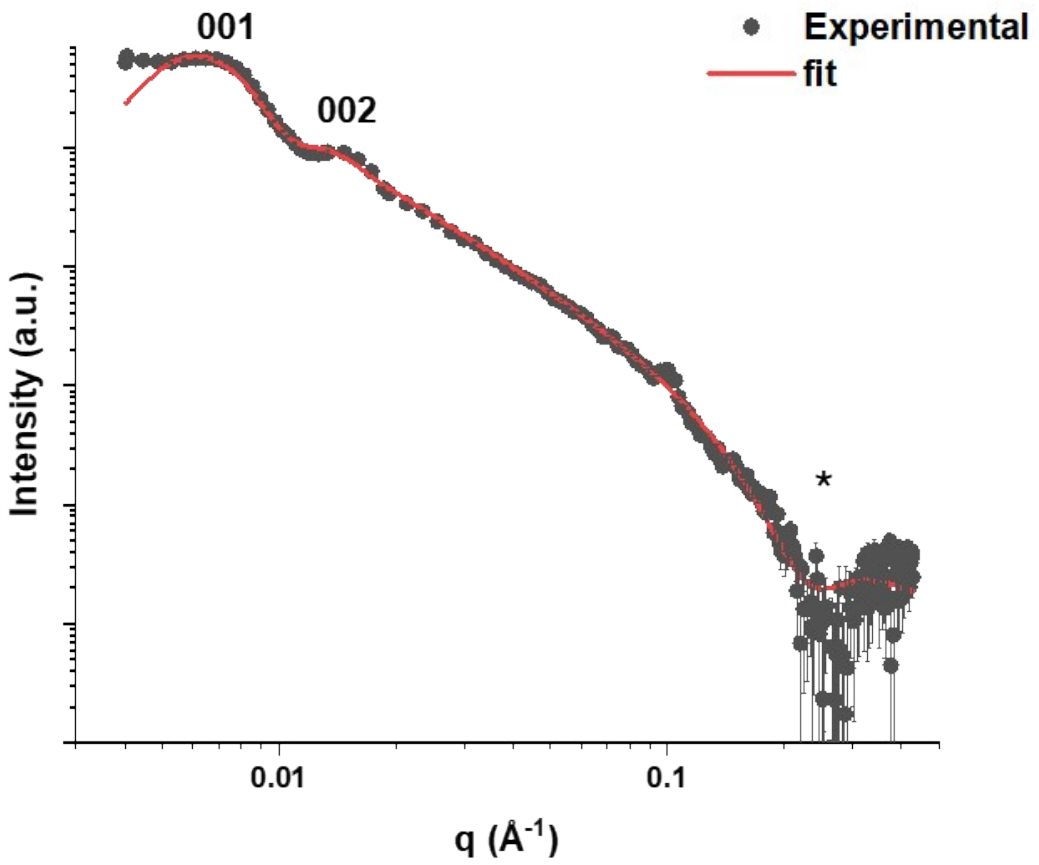

Figure S1. SAXS pattern of the nematic liquid crystal of double stacks at a concentration of 4wt%. The rational *00l* series indicates the spacing between the nanosheets to be 85 nm. * labels the structure factor minimum, indicating the characteristic thickness of the platelets to be 2.5 nm.

Maghemite nanoparticle characterization

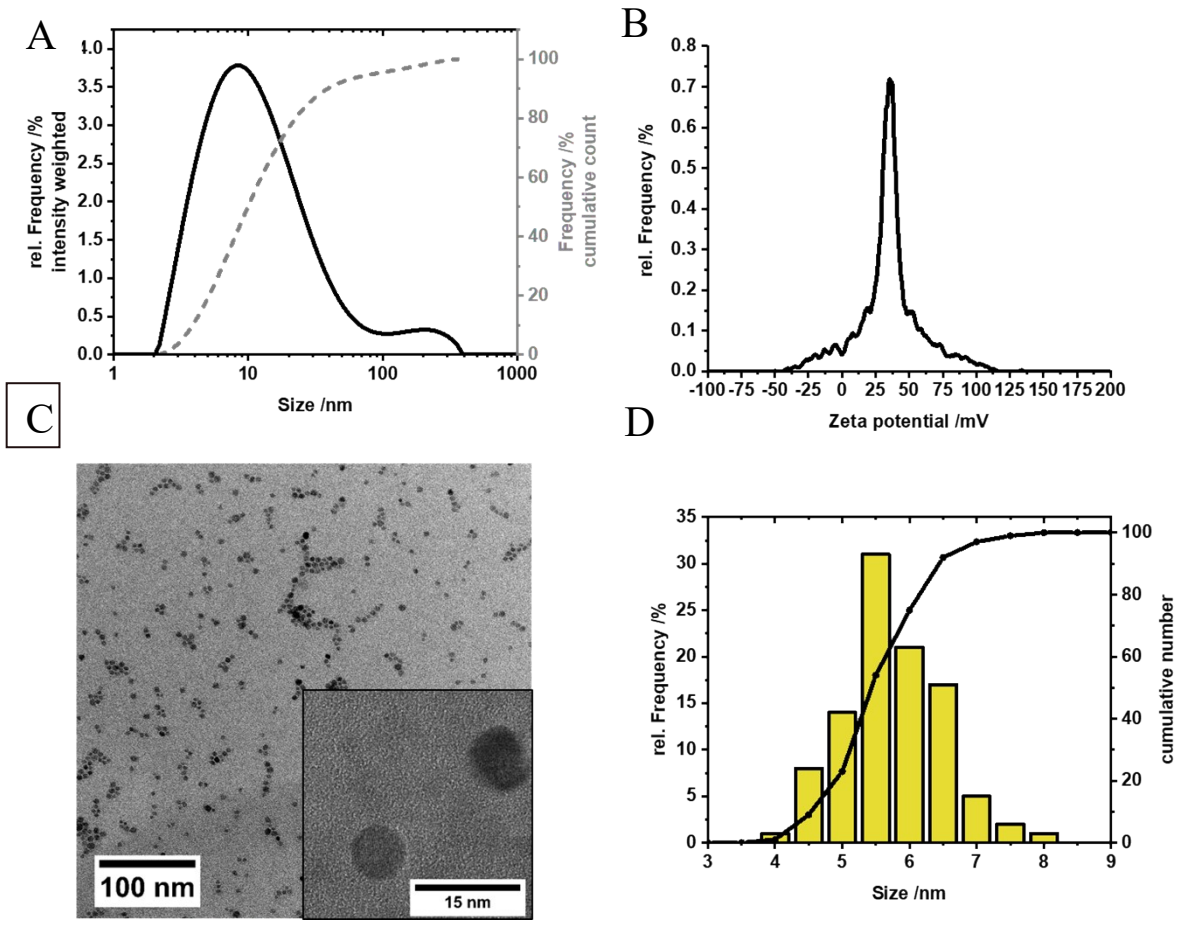

Figure S2. Characterization of nanoparticles. (A) hydrodynamic diameter according to DLS measurement. (B) zeta potential at pH 7 of y-Fe_2O_3 nanoparticles. (C) TEM image of y-Fe_2O_3 nanoparticles. (D) histogram of the core sizes of 100 particles.

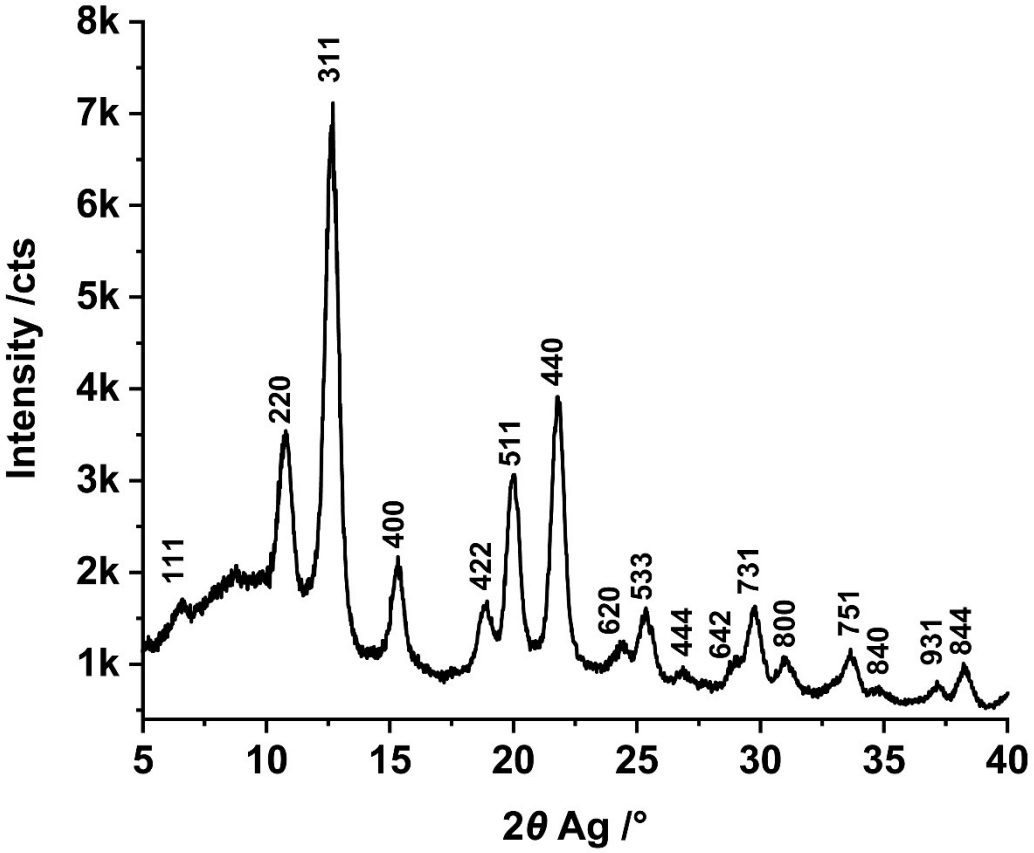

XRD pattern of y-Fe_2O_3

Figure S3. Wide angle PXRD using Ag-K_α (λ = 0.5594075 Å) radiation of y-Fe_2O_3 nanoparticles

Mößbauer spectroscopy of γ-Fe_2O_3

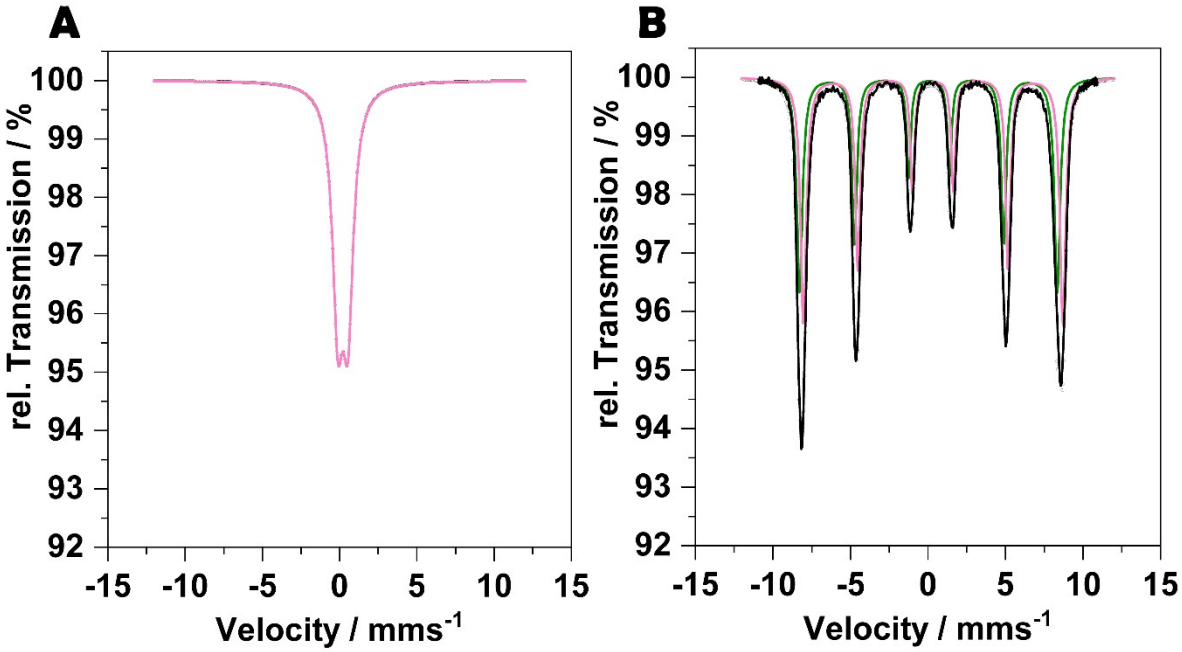

Figure S4. (A) Room temperature Mößbauer spectrum showing only one quadrupole doublet. (B) 4.2 K Mößbauer spectrum with two sextets for Fe^{3+} in tetrahedral sites (green) and octahedral sites (pink).

To additionally confirm the formation of the γ-Fe_2O_3 we performed the Mößbauer spectroscopy, because the standard XRD peaks of γ-Fe_2O_3 and Fe_3O_4 are almost identical. The RT spectrum showed only one quadrupole doublet due to fast superparamagnetic relaxation processes that is characteristic for small sized iron oxide nanoparticles (Figure S4 A). The spectrum recorded at 4.2 K showed two sextets with nearly identical hyperfine fields and nearly no quadrupole interaction (Figure S4 B). The isomeric shifts of 0.05 mm·s^{-1} and 0.33 mm·s^{-1} corresponded to the tetrahedral and octahedral sites of Fe^{3+}, respectively. Fe^{2+} that would indicate a magnetite phase could not be observed.[1, 2]

XRD pattern of NH_4^+/Na^+ ordered heterostructures also named ordered interstratification (OI)

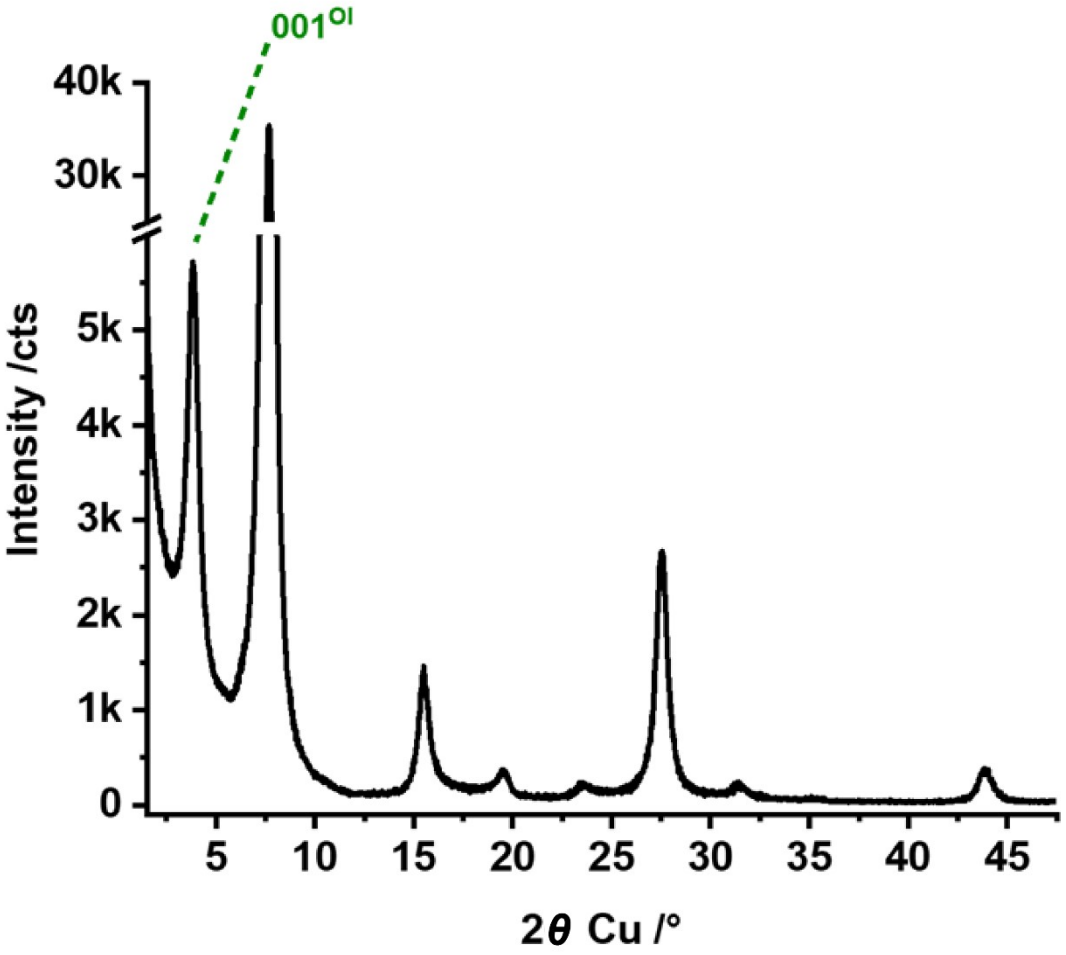

Figure S5. Wide angle PXRD of the ordered interstratification (OI) of strictly alternating Na^+ and NH_4^+ layers in synthetic hectorite. The sample was equilibrated in an atmosphere with 43% relative humidity.

AFM of double stacks

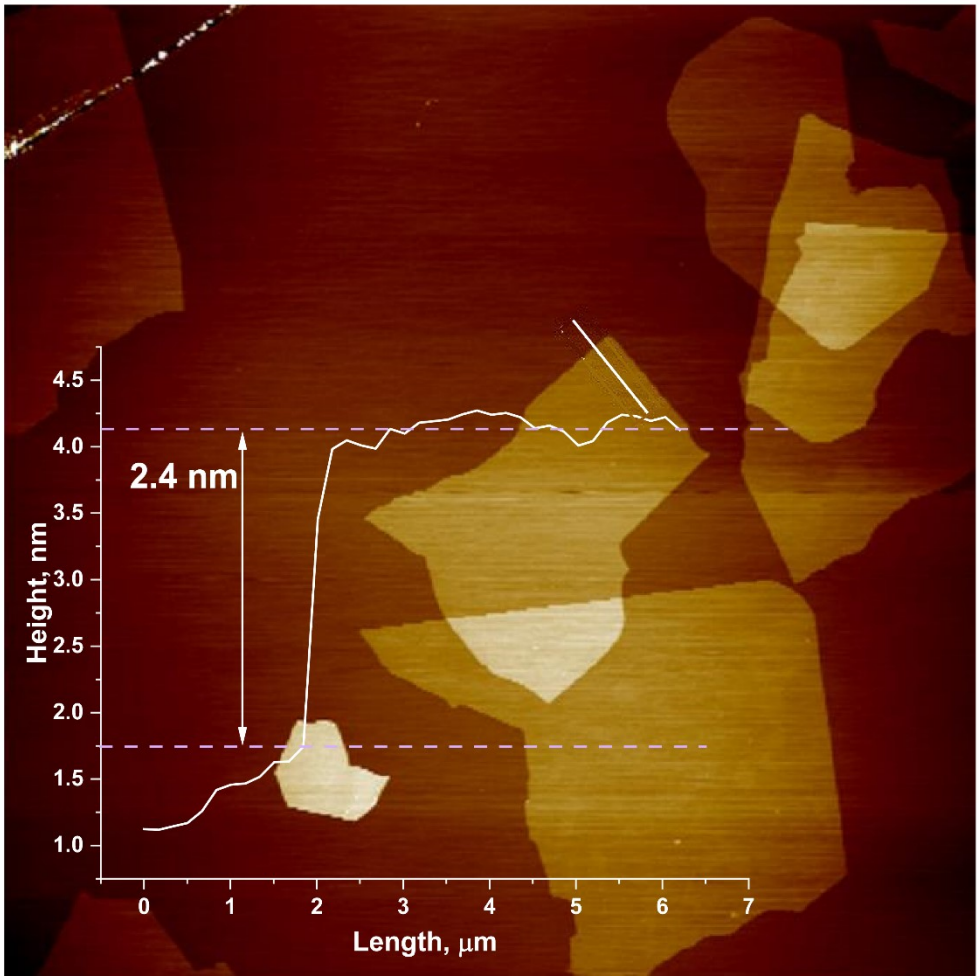

Figure S6. Representative, topographical AFM image of double stacks. A height profile shows a platelet thickness of 2.4 nm.

ICP-OES

Table S1. Elemental composition according to ICP-OES.

Element	**Weight fraction of the element [%]**		
Nominal Fe_2O_3	*16 wt%*	*30 wt%*	*45 wt%*
Fe	11.9	21.5	31.8
Mg	13.4	11.2	8.8
Fe_2O_3 wt%[a]	17	31	46
Nominal Formula[b]	$(Fe_2O_3)_{0.46}Li_{0.31}$ $(Mg_{2.5}Li_{0.5}Si_4O_{10}F_2)$	$(Fe_2O_3)_{1.05}Li_{0.31}$ $(Mg_{2.5}Li_{0.5}Si_4O_{10}F_2)$	$(Fe_2O_3)_{1.95}Li_{0.31}$ $(Mg_{2.5}Li_{0.5}Si_4O_{10}F_2)$

[a] Assuming an stoichiometric composition of Fe_2O_3 the weight fraction of maghemite nanoparticles is calculated from the Fe wt%.

[b] Then the nominal formula was calculated to be $(Fe_2O_3)xLi_{0.31}(Mg_{2.5}Li_{0.5}Si_4O_{10}F_2)$. Si was not detected directly via ICP-OES. The amount of Si was rather calculated assuming the atomic ratio of Mg to Si of 2.5:4 as required by the hectorite-composition.

Top-view TEM MDS 16.6

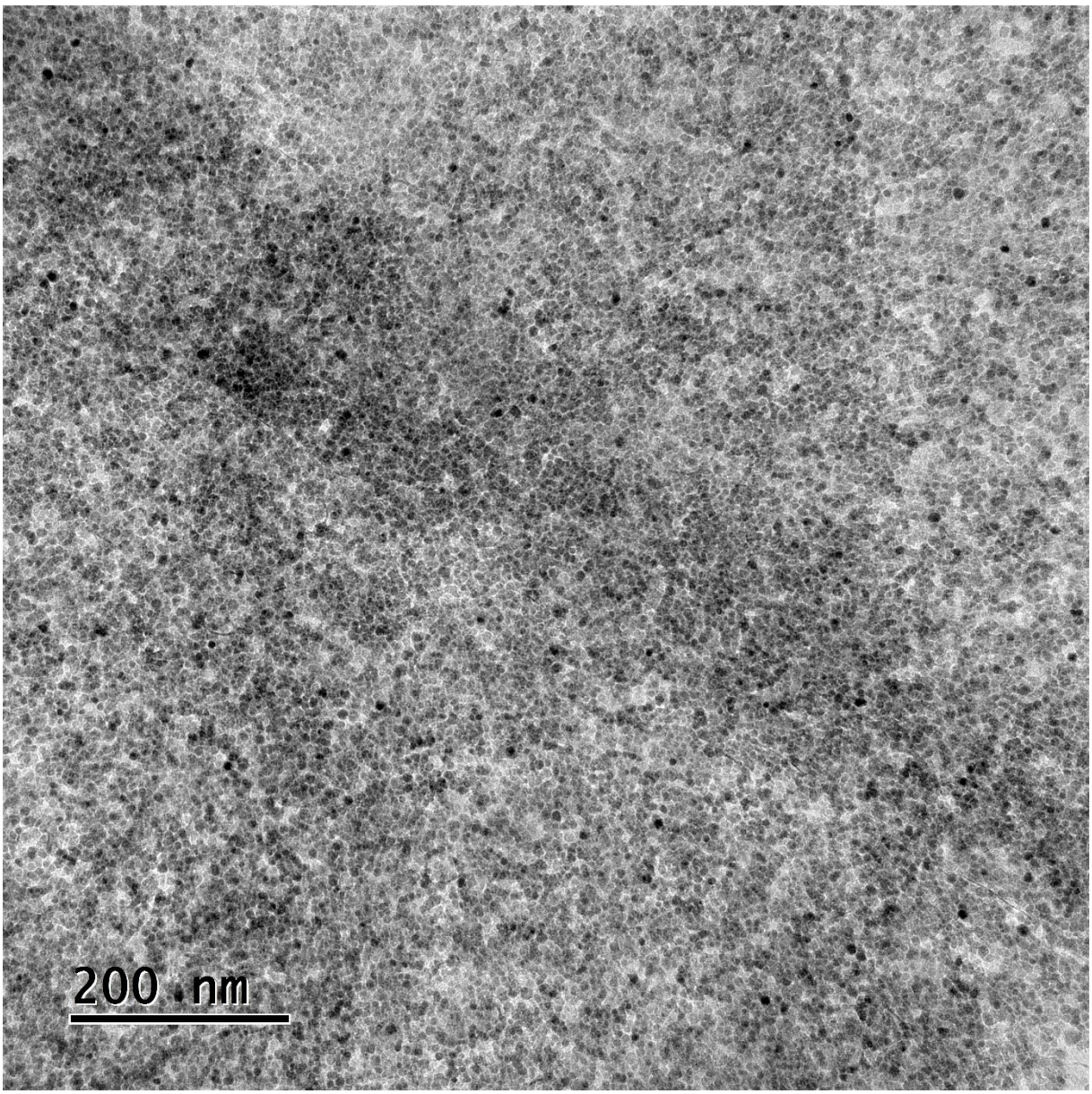

Figure S7. TEM image of top view of the MDS 16.6.

BET

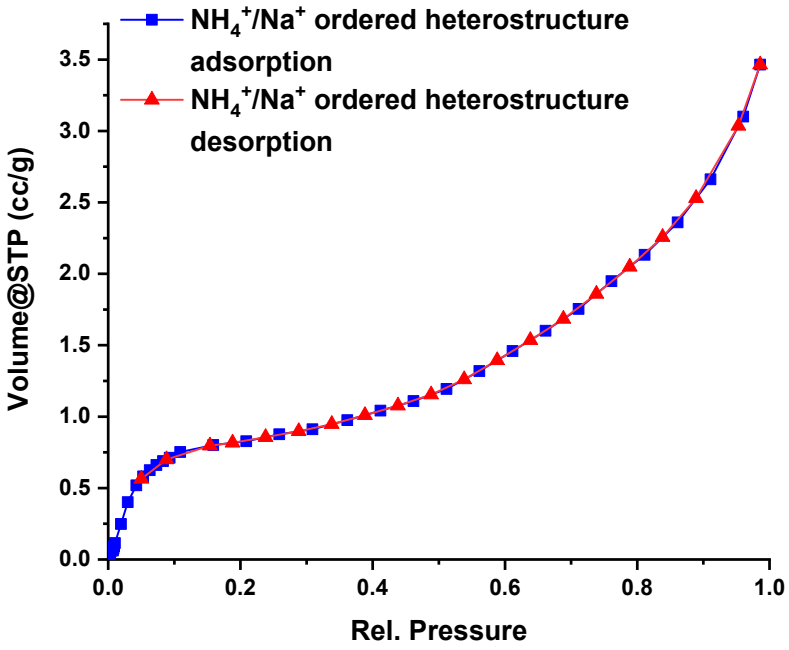

Figure S8. Nitrogen adsorption-desorption isotherms of the NH_4^+/Na^+ ordered heterostructures.

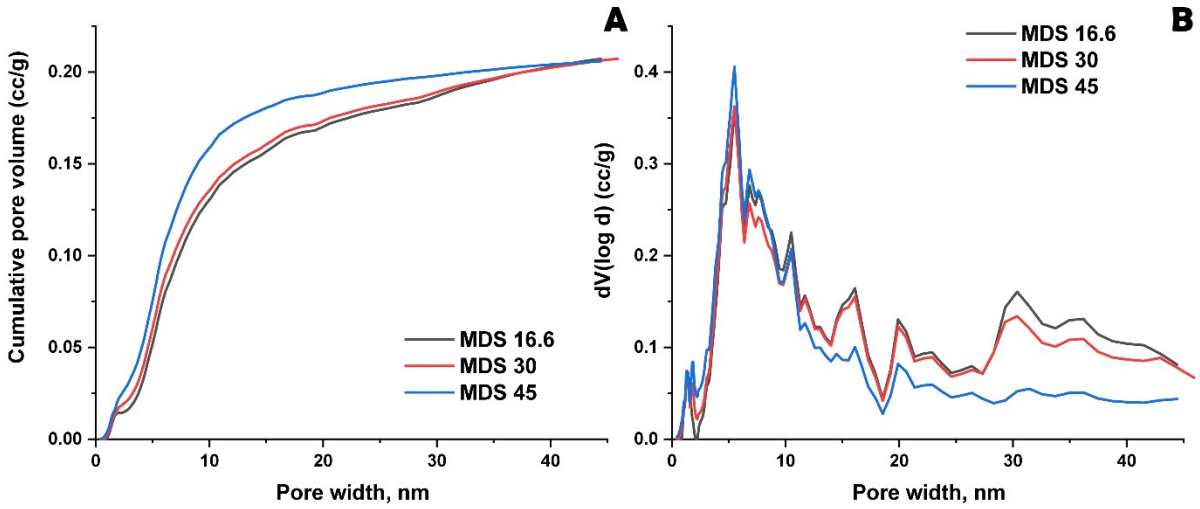

Figure S9. Pore width analysis of nitrogen physisorption isotherms taken at 77 K derived by applying the DFT kernel for MDS 16.6, MDS 30, MDS 45. (A) Cumulative pore volumes (B) Pore size distributions.

Grayscale analysis of a TEM micrograph taken for a cross section of restacked

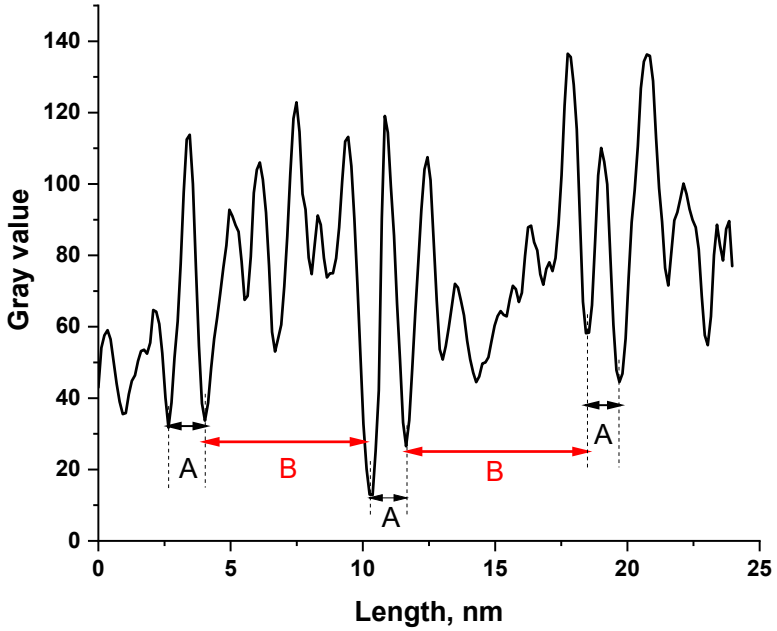

MDS

Figure S10. Grayscale analysis of a TEM micrograph taken for a cross section of restacked MDS showing the periodic arrangement of the material with characteristic lengths A = 1.3 nm corresponding to the distance between the centres of two silicate nanosheets and B = 6.54 nm corresponding to the diameter of nanoparticles sandwiched between two nanosheets.

Orientation order analysis

The orientation order parameter was calculated using the following formula based on the description from Lovell and Mitchel by averaging over the second Legendre polynomial.[3]

$$S = -2 \cdot \frac{\int_0^{\frac{\pi}{2}} I(\phi) \cdot 1/2 \cdot (3\cos^2\phi - 1) \cdot \sin\phi d\phi}{\int_0^{\frac{\pi}{2}} I(\phi) \cdot \sin\phi d\phi}$$

S is the order parameter, ϕ is the azimuthal angle (*y* axis corresponds to ϕ = 0) $I(\phi)$ is the intensity at ϕ. In order to minimize smearing effects from the collimation of the SAXS instrument the $I(\phi)$ was averaged in the range of 0.03nm^{-1}< q <0.14nm^{-1}. The order parameter has a value of S=0.7 which is very well ordered with respect to the director given by the magnetic field.

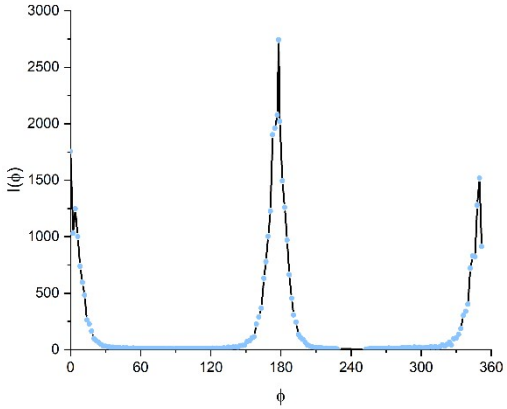

Figure S11. The $I(\phi)$ plot of the magnetically oriented sample used to calculate the order parameter.

Data reduction for SAXS of the oriented sample and fit with 2D structure factor

The sample was filled in a 1 mm Hilgenberg glass capillary and inserted in a homemade sample holder consisting of two fixed permanent magnets, left and right of the vertically orientated capillary. The field strength on the sample position is ~0.9 T. For the measurements without field another sample holder was used. For both a separate water background was measured as well.

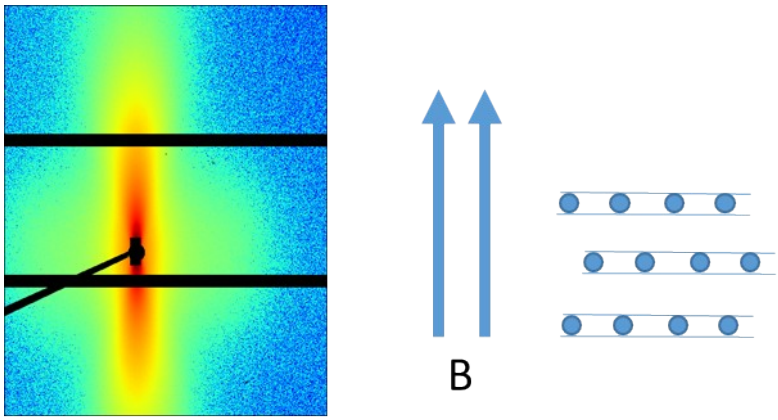

Figure S12. Left: 2D SAXS pattern in magnetic field, middle: direction of the magnetic field, right: direction of the stacks.

Data reduction for SAXS of the oriented sample and fit with 2D structure factor

In order to be able to properly account for the anisotropy in the samples scattering the back ground was subtracted in 2D and subsequently the radial average was either along the nematic director or perpendicular to it. To do that we chose the width of the peaks in the $I(\phi)$ plots to define the regions of interest. The radial averaged data from the three detector distances was scaled to measurement time, transmission as well sample thickness and put on absolute scale. For the highly oriented sample we got two scattering curves.

This enables us to separate the scattering of the sheets from the particle scattering. As the particles are isotropic they scatter to all angles even when the much stronger scattering sheets

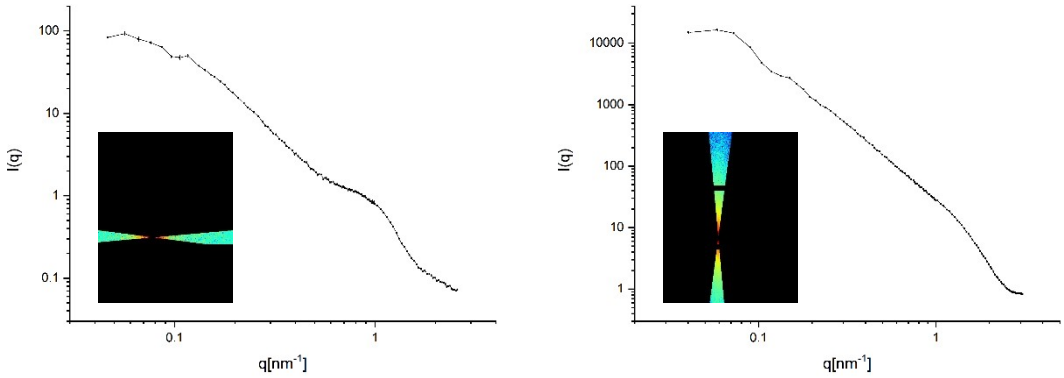

are oriented due to the magnetic field.

Figure S13. Left: radial averaged scattering along the nematic director with particle scattering visible next to a contribution at low q from sheets which are not perfectly oriented. Right: radial averaged scattering perpendicular the nematic director where the contribution from the sheets is a hundred times higher than on the left side.

Data reduction for SAXS of the oriented sample and fit with 2D structure factor

In order to separate the excess particle scattering from the sheets we used the I(q) scaling at medium 0.3>q<0.4 to shift both curves on top of each other.

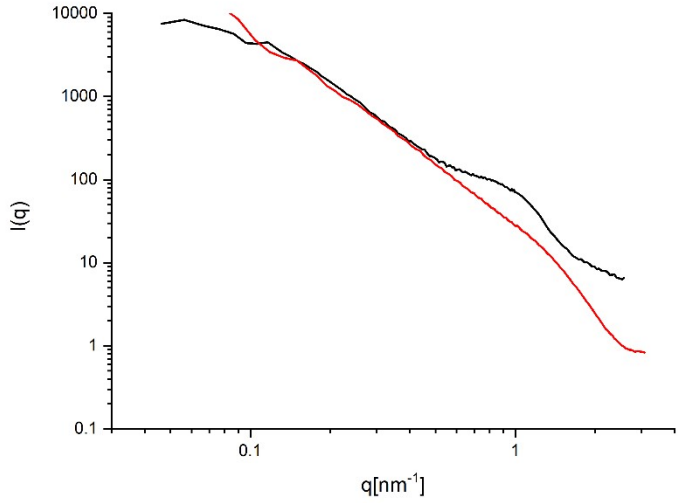

Figure S14. Shifted radial average along the nematic director so that the intermediate q values overlap.

By subtracting the red from the black curve the excess particle scattering within the sheets is extracted. This is possible because at high q the red curve is dominated by the sheet form factor and the nice $I(q)\sim q^{-2}$ scaling at intermediate q values for both curves. The resulting scattering curve represents the scattering from the particles within the double stacks only.

We also were able to fit this data with a model for polydisperse spheres also taking into account the 2D Percus Yevick structure factor for hard spheres.[4] The fit results in a particle radius of 2.5nm±0.5nm and a 2D packing fraction of 0.4. The particle radius fits very good with the TEM and DLS results as far as the packing fraction within the layer goes it is an average value over the whole sample and seems reasonably high.

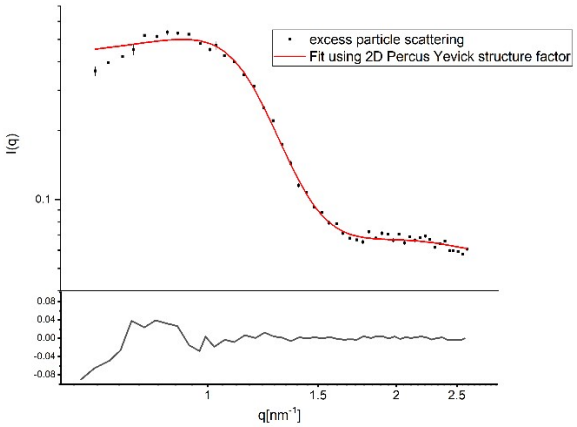

Figure S15. Excess particle scattering with the fit using a polydisperse sphere model with 2D PY structure factor.

Photographs of nematic texturing

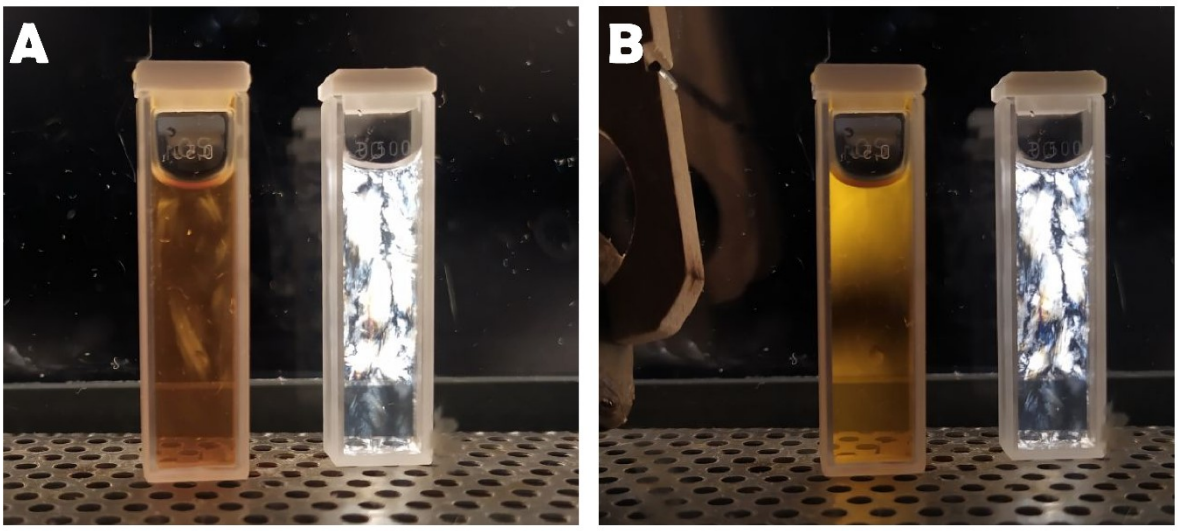

Figure S15. Photographs of nematic phases of DS (right cuvette) and MDS (left cuvette) without (A) and with (B) applied magnetic field in cross-polarized light.

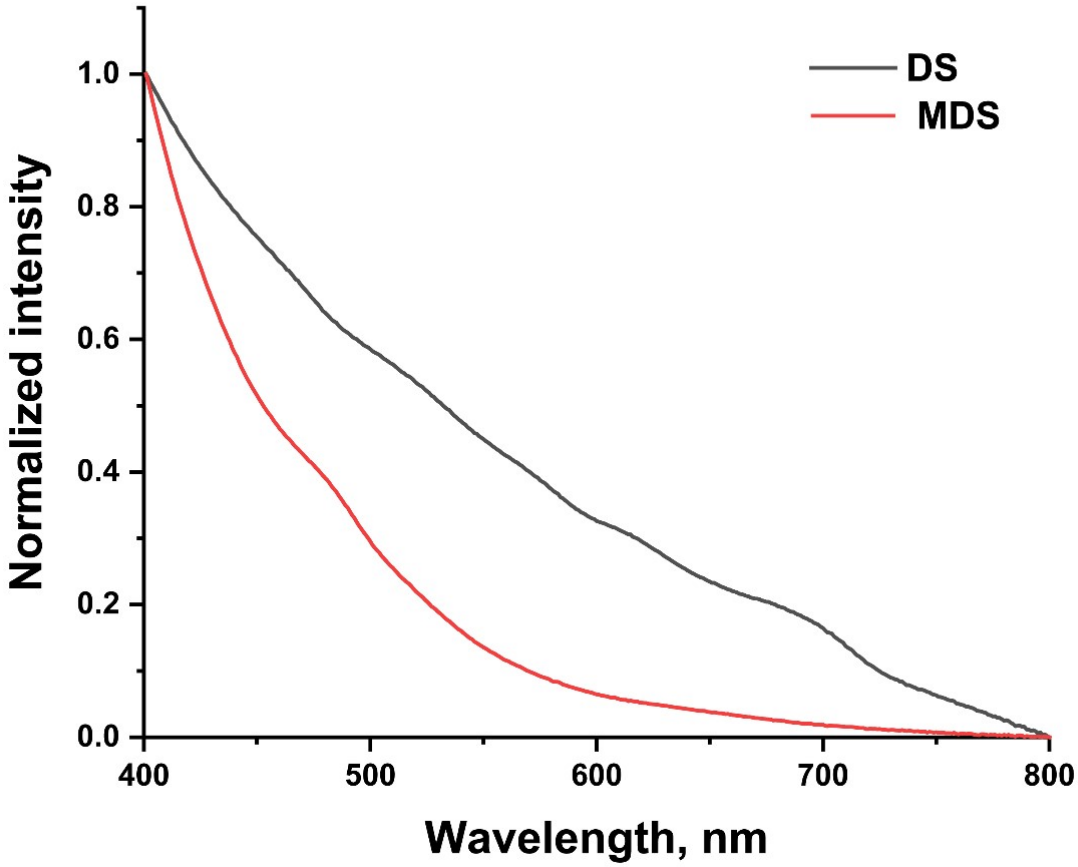

Figure S16. UV-vis spectra of nematic phases DS (black, 0.3 wt%) and MDS (red, 0.15 wt%).

References

1. K. Ament, D. R. Wagner, F. E. Meij, F. E. Wagner and J. Breu, *Z. Anorg. Allg. Chem.*, 2020, **646**, 1110–1115.
2. F. J. Berry, S. Skinner and M. F. Thomas, *J. Phys.: Condens. Matter*, 1998, **10**, 215–220.
3. R. Lovell and G. R. Mitchell, *Acta Cryst. A*, 1981, **37**, 135–137.
4. Y. Rosenfeld, *Phys. Rev. A*, 1990, **42**, 5978–5989.